

PAPER • OPEN ACCESS

## Properties of ns-laser processed polydimethylsiloxane (PDMS)

To cite this article: P A Atanasov *et al* 2016 *J. Phys.: Conf. Ser.* **700** 012023

View the [article online](#) for updates and enhancements.

### You may also like

- [Laser-induced breakdown spectroscopy analyses of tungsten surfaces](#)  
D Nishijima, E M Hollmann, R P Doerner et al.
- [Laser modification of Au–CuO–Au structures for improved electrical and electro-optical properties](#)  
Shuo Zheng, Walter W Duley, Peng Peng et al.
- [A comparative study of emission efficiencies in low-pressure argon plasmas induced by picosecond and nanosecond Nd:YAG lasers](#)  
Alion Mangasi Marpaung, Muliadi Ramli, Rinaldi Idroes et al.

**ECS** The Electrochemical Society  
Advancing solid state & electrochemical science & technology

**241st ECS Meeting**

Vancouver, BC, Canada. May 29 – June 2, 2022

ECS Plenary Lecture featuring  
**Prof. Jeff Dahn,**  
**Dalhousie University**

**Register now!**

## Properties of ns-laser processed polydimethylsiloxane (PDMS)

P A Atanasov<sup>1,4</sup>, N E Stankova<sup>1</sup>, N N Nedyalkov<sup>1</sup>, T R Stoyanchoy<sup>1</sup>,  
Ru G Nikov<sup>1</sup>, N Fukata<sup>2</sup>, J W Gerlach<sup>3</sup>, D Hirsch<sup>3</sup> and B Rauschenbach<sup>3</sup>

<sup>1</sup>Emil Djakov Institute of Electronics, Bulgarian Academy of Sciences,  
72 Tsarigradsko Chaussee, 1784 Sofia, Bulgaria

<sup>2</sup>International Center for Materials for Nano-Architectonics (MANA), National  
Institute for Materials Science (NIMS), 1-1 Namiki, Tsukuba 305-0044, Japan

<sup>3</sup>Leibniz Institute of Surface Modification (IOM),  
Permoserstrasse 15 D-04318 Leipzig, Germany

E-mail: paatanas@ie.bas.bg

**Abstract.** The medical-grade polydimethylsiloxane (PDMS) elastomer is a widely used biomaterial in medicine and for preparation of high-tech devices because of its remarkable properties. In this work, we present the experimental results on drilling holes on the PDMS surface by using ultraviolet, visible or near-infrared ns-laser pulses and on studying the changes of the chemical composition and structure inside the processed areas. The material in the zone of the holes is studied by XRD,  $\mu$ -Raman analyses and 3D laser microscopy in order to obtain information on the influence of different processing laser parameters, as wavelength, fluence and number of consecutive pulses on the material transformation and its modification.

### 1. Introduction

Polydimethylsiloxane (PDMS) belongs to the group of polymeric materials called silicones possessing one common characteristic – the polymer backbone is composed by an alternate succession of Si and O atoms joined together via strong, covalent inter-atomic bonds. The Si atoms are coupled to two adjacent O atoms and two organic radicals. PDMS is among the most popular technical polymeric materials due to its advantageous properties: mechanical flexibility and stability; non-toxicity; permeability to gasses; chemical and biological inertness; high dielectric constant and breakdown field; optical transparency in the ultraviolet (UV) ÷ visible (VIS) regions of the spectra; high biocompatibility and biostability; very hydrophobic; simple and inexpensive fabrication.

PDMS has been widely used in the fabrication of various micro-electro-mechanical systems (MEMS) [1-6] and flexible microelectrode arrays for monitoring and/or stimulation of neural activity [8-10]. The hydrophilic, hydrophobic recovery and surface energy of the material have been studied [11]. Furthermore, the cytotoxicity and antibacterial activity of the material has also been assessed; the results obtained revealed that the PDMS surface modifications performed do not affect the material's biocompatibility, but decrease their hydrophobic character and bacterial adhesion. Thus, the modification or structure formation on the surface of the PDMS is of great importance and growing research interest.

<sup>4</sup> To whom any correspondence should be addressed.



The use of laser radiation offers a useful approach to processing and selective surface functionalization of the PDMS material. In particular, ns-laser pulses (e.g., KrF, ArF and F<sub>2</sub>) have been applied to the fabrication of optical elements [12], modification of optical properties [13] and surface processing or functionalization [2, 8, 10]. KrF excimer laser processing of flexible silicone rubber has been used to photo-decompose its surface or to change the surface relief [2, 8, 14, 15]. Information on the changes of the PDMS structures fabricated by ns-laser pulses has been typically obtained by  $\mu$ -Raman measurements [8]. Laser irradiation can obviously induce breaking of the chemical bonds, but it can also be used in the ablation mode to micro- or nano-structuring the polymer surface, thus enhancing the adhesion of a metal [14, 15].

Nowadays, UV and VIS fs- or ns-laser irradiation of the PDMS-elastomer under ambient conditions has been proven to be an easy and powerful method for surface micromachining in order to fabricate tracks and structures with surface activation without altering its bulk properties [16-18]. Samples of the PDMS elastomer processed by UV, VIS and NIR fs- and ns-laser pulses have been investigated [14-18]. A limited number of laser processed areas has been viewed by SEM and optical microscopy. Selective Pt or Ni metallization of the laser-processed traces have been produced successfully via electro-less plating. The metallization process is not sensitive to the time interval after the laser treatment. The DC resistance has been measured to be as low as 0.5  $\Omega$ /mm [17]. The present paper reports the results on the changes in the PDMS elastomer properties inside the holes produced as a result of multi-pulse ns-laser ablation at the wavelengths of 266, 355, 532 and 1064 nm. The laser fluence and number of consecutive pulses were varied. The laser-processed areas were studied by laser microscopy, XRD and  $\mu$ -Raman spectroscopy. The as-processed areas were successfully metallized by Ni via electro-less plating.

## 2. Experimental

180  $\mu$ m thick medical grade PDMS-elastomer sheets (MED 4860) were irradiated by the fundamental harmonic (NIR) ( $\lambda = 1064$  nm), and the 2<sup>nd</sup> ( $\lambda = 532$  nm), 3<sup>rd</sup> ( $\lambda = 355$  nm) and 4<sup>th</sup> ( $\lambda = 266$  nm) harmonics of a Q-switched Nd:YAG laser (pulse duration of 15 ns and repetition rate of 10 Hz) in air at ambient temperature. The samples were mounted on a microcontroller-driven, stepper-motor operated X–Y table. The laser beam was focused by a lens with a focal length of 22 cm. The micro-holes were produced without perforating the foil by up to 110 consecutive laser pulses. The laser fluence was varied at the different wavelengths. The corresponding data of the laser processing parameters are presented in table 1.

**Table 1.** Summary of the laser processing parameters.

Wavelength (nm)	266	355	532	1064
Laser Fluence (J cm <sup>-2</sup> )	0.1 ÷ 1.0	1.0 ÷ 2.5	3.5 ÷ 5.0	8.0 ÷ 13.0

The areas of the holes produced were viewed and their physical dimensions measured by a VK-9700 K Color 3D Laser Microscope (KEYENCE, Japan). The crystalline properties were studied by an XRD – ULTIMA IV X-Ray Diffractometer (RIGAKU, Japan), while the chemical modifications were analyzed at different points of the holes by a  $\mu$ -Raman Spectrometer – RMS-310 (Photon Design, Japan) with laser excitation at 532 nm. The spectrometer has a resolution of 0.2 cm<sup>-1</sup> and image dimension <1  $\mu$ m<sup>2</sup>. Additionally, continuous trenches with dimension of 12×3 mm<sup>2</sup> and different depths were prepared at various laser fluences in order to investigate the laser-processed area by 1° grazing incidence XRD.

## 3. Results and discussions

### 3.1. XRD analyses

The results from the XRD analyses are presented in figure 1. Figure 1 a) depicts the XRD spectrum of the non-processed PDMS. The spectrum is similar to that reported in reference [11].

As it is illustrated in figure 1 b), all diffraction patterns are similar, presenting two diffraction halos: a first and larger one located at around 12.3° and a second, smaller and broader one, at 22.2°. These results indicate that the microstructure of the samples is amorphous and that the ns-laser processing does not change the bulk properties of the base material. Additionally, the intensity of the material treated by UV ( $\lambda = 355$  nm) ns-laser pulses has about twice as high intensity compared to the other wavelengths applied, which is probably related to the better ordering of the material processed.

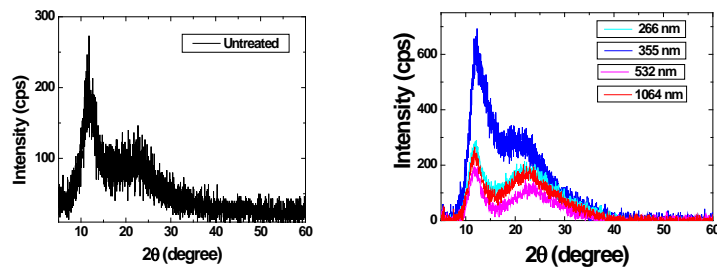


**Figure 1.** XRD spectra of the unprocessed – a) and ns-laser processed area of PDMS – b).

### 3.2. Color microscope views of the holes

The laser produced micro holes were viewed by a 3D color laser microscope – figure 2 a) – c).

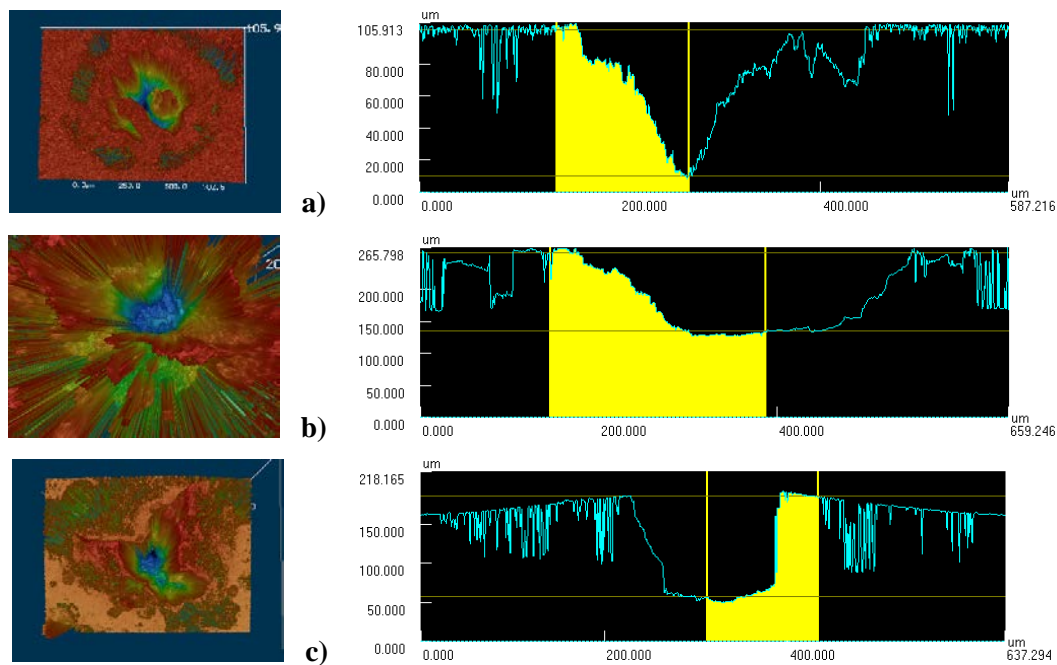


**Figure 2.** a), b) and c) show photographs and profiles of some of the holes produced by a ns-laser: a) 266 nm, 110 pulses; b) 532 nm, 33 pulses; c) 1064 nm, 33 pulses.

Due to the multimode structure of the laser beam, the holes' profiles are not uniform. This leads to the production of holes with an inhomogeneous structure, especially in the cases of a higher number of consecutive incident pulses. The peculiarities of the properties at different points of the areas processed resulted from the different energy density inside the laser beam, i.e. the existence of some “hot” spots. These differences were clearly expressed in the Raman studies. It is worth noting that when producing tracks by a ns-laser, the quality of the tracks was better due to the equalization of the processing after overlapping of a large number of the pulses (> 30) during the slow movement of the X-Y table.

However, a further effort was needed in order to improve the quality of the laser-beam profile. In this respect, a laser beam equalizer was introduced and the results will be the subject of further investigations.

### 3.3. Raman spectroscopy inside the holes

The  $\mu$ -Raman spectra taken from the center or periphery of the holes are presented in figure 3 a) - d). Figure 3 a) – c) correspond, respectively, to the pictures given in figure 2 a) - c). In addition, figure 3 e) depicts the spectrum of the native PDMS given as a comparison. It clearly shows that the appearance of a crystalline Si peak is observed for all laser wavelengths applied. The intensity of the crystalline Si peak increases with the laser fluence and the number of consecutive pulses. The spectra in figure 3 a) – d) illustrate a well-defined change of the chemical composition regardless of the laser wavelength used for processing. An extra peak at  $\sim 512 \div 520 \text{ cm}^{-1}$ , assigned to crystalline silicon (c-Si), is observed after ns-laser processing. Simultaneously, the intensity of the Si-O-Si peak at  $488 \text{ cm}^{-1}$ , typical for the native PDMS, decreases. Probably, this is a consequence of the reduction of the Si-O-Si bonds by breaking of the Si-O bond and, as a result, Si crystallites are formed. Also, the intensities of the Si-O-Si symmetric stretching at  $488 \text{ cm}^{-1}$ , the Si-CH<sub>3</sub> symmetric rocking at  $685 \text{ cm}^{-1}$ , the Si-C symmetric stretching at  $709 \text{ cm}^{-1}$ , the CH<sub>3</sub> asymmetric rocking, the +Si-C asymmetric stretching at  $787 \text{ cm}^{-1}$ , and the CH<sub>3</sub> symmetric rocking at  $859 \text{ cm}^{-1}$  modes decrease, which could contribute to the c-Si formation as well.

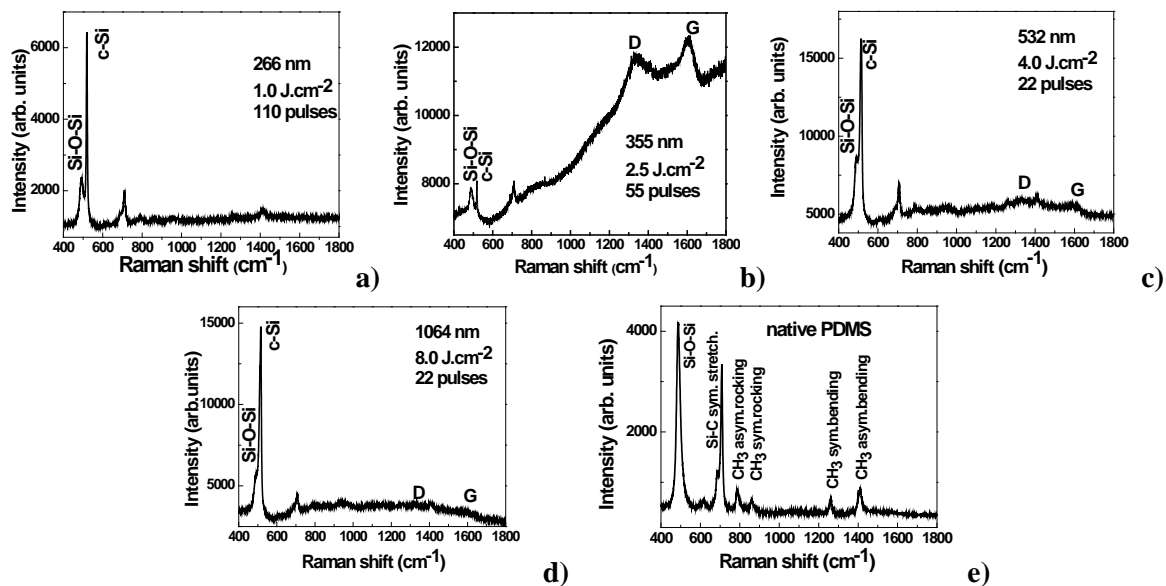


**Figure 3.**  $\mu$ -Raman spectra of the holes as in Fig. 2: a) 266 nm – at a point inside the hole produced; b) 355 nm – at a point inside the hole produced; c) 532 nm – at the center of the hole; d) 1064 nm – at the center of the hole. e) the spectrum of the native (non-processed) PDMS.

Two wide peaks in the ranges of  $1320 \div 1336 \text{ cm}^{-1}$  and  $1590 \div 1615 \text{ cm}^{-1}$  are observed in the Raman spectra of some points of the areas treated with both UV lights, which are well expressed at number of pulses  $> 33$ . These two peaks are much weaker when the PDMS is irradiated by VIS and NIR wavelengths. In some cases, the high signal of these peaks' tails hinders the expression of the other Raman features. When the peak of crystalline Si is well expressed, these two peaks are almost hidden (figure 3 a)).

As it is known, the amorphous carbon contains a mixture of  $sp^3$ ,  $sp^2$  and  $sp^1$  sites. The Raman spectrum taken by VIS excitation contains two peaks – D and G modes, which appear at  $\sim 1360$  and  $1560 \text{ cm}^{-1}$  [19]. These peaks dominate, because the  $sp^2$  sites have cross-sections much higher than that

of the  $sp^3$ . However, in the case of a high number of  $sp^3$  sites (which are related to the diamond phase) the D peak appears at  $1332\text{ cm}^{-1}$ . It is worth noting that the position of the D peak could be extended in the range between  $1300$  and  $1350\text{ cm}^{-1}$  if the phase is mixed with the hexagonal and cubic diamond [20]. Usually, this peak is broadened and lowered because of the phonon confinement at VIS excitation. It has also been shown that carbon materials, which contain simultaneously  $sp^2$  and  $sp^3$  phases, reveal a shift of the G band over the  $1600\text{ cm}^{-1}$  [19, 21]. Hence, it could be concluded that the laser treated areas of PDMS, especially by both UV wavelengths, contain a significant fraction of  $sp^3$  carbon bonds.

The micro-Raman analysis also showed that local chemical modifications (i.e. silicone decomposition) occurred after the laser processing of the PDMS, irrespective of the corresponding wavelengths used. This behavior is due to the rather significant influence of the laser fluence and/or the number of the pulses rather than that of the wavelength. The formation of inorganic products like Si and C is responsible for the chemical activation of the surface, which is expected to influence significantly the nucleation and the growing rate of the metal layer (Ni or Pt) during the following process of metallization.

## 6. Conclusions

Results on processing of a medical grade PDMS elastomer by UV, VIS and NIR ns-laser pulses are presented. A change of the chemical composition of the areas processed (holes) is observed and compared to the non-processed material. An XRD study of the laser-processed PDMS material at NIR, VIS and UV lights is conducted for the first time. The results obtained can be summarized as follows: i) no crystalline phases caused by laser treatment are observed in the XRD spectra; very broad “peaks” are related to the amorphous phases of the material; ii) for all wavelengths, the appearance of a crystalline Si peak is observed in the  $\mu$ -Raman spectra; its intensity increases with the laser fluence and the number of pulses; iii) amorphous carbon containing  $sp^2$  and  $sp^3$  sites is formed during the laser activation of the surface; iv) the local chemical decomposition is a complex function of the laser fluence, the number of the pulses (incubation) and the wavelength; v) the quality of the laser beam is found to be very important for the processing and functionalization of the PDMS surface for further metallization.

## Acknowledgements

The financial support is acknowledged of the Bulgarian National Science Fund under project T02/24 “New advanced method for processing nanocomposite materials for creation of microsystems for medical and high-tech applications” and of the German-Bulgarian bilateral project 01/1 “Ion beam and laser techniques for surface nanostructuring of different materials and application to high resolution analyses (SERS)”.

## References

- [1] Editorial Overview 2009 Lasers in surface science *Current Opinion in Solid State and Materials Science* 1-3
- [2] Laude L, Rowley A, Humayun M and Weiland J 2008 *US Patent* US 2008/10305320 A1
- [3] McDonald J C, Duffy D C, Anderson J R, Chiu D T, Wu H, Schueller O J and Whitesides G M 2000 *Electrophoresis* **21**/1 27
- [4] Makamba H, Kim J H, Lim K, Park N and Hahn J H 2003 *Electrophoresis* **24**/21 3607
- [5] 2004 *Silicon Compounds: Silanes and Silicones* (Gelest, Inc. Morrisville PA) 560
- [6] Hermanson G T, Mallia A K and Smith P K. 1992 *Immobilized Affinity Ligand Techniques* (Academic Press San Diego CA) 454
- [7] Okoshi M, Li J and Herman P R 2005 *Opt. Lett.* **30**/20 2730
- [8] Dicara C, Robert T, Kolev K, Dupas-Bruzek C and Laude L D 2003 *Proc. SPIE* **5147** 255
- [9] Laude L D 1997 *US Patent* No 5599592
- [10] Dupas-Bruzek C, Robbe O, Addad A, Turrell S and Derozier D 2009 *Appl. Surf. Sci.* **255**

8715

- [11] Ferreira P, Carvalho A, Correia T R, Bernardo, Antunes P, Correia I J and Alves P 2013 *Sci. Technol. Adv. Mater.* **14** 055006
- [12] Okoshi M, Li J and Herman P R 2005 *Opt. Lett.* **30** 2730
- [13] Okoshi M, Sekine D, Inoue N and Yamashita T 2007 *Jpn. J. Appl. Phys. Part 2* **46** L356
- [14] Laude L D 1997 *U.S. Patent* N 5.599.592
- [15] Dini J W 1997 *Met. Finish.* **95** 10
- [16] Atanasov P A, Nedyalkov N N, Valova E I, Georgieva Zh S, Armanyanov S A, Kolev K N, Amoroso S, Wang X, Bruzzese R, Sawczak M and Śliwiński G. 2014 *J. Appl. Phys.* **116**/2 023104
- [17] Stankova N E, Atanasov P A, Nedyalkov N N, Stoyanchov T R, Kolev K N, Valova E I, Georgieva J S, Armanyanov St A, Amoroso S, Wang X, Bruzzese R, Grochowska K, Śliwiński G, Baert K, Hubin A, Delplancke M P and Dille J 2015 *Appl. Surf. Sci.* **336** 321
- [18] Armanyanov S, Stankova N E, Atanasov P A, Valova E, Kolev K, Georgieva J, Steenhaut O, Baert K and Hubin A 2015 *Nucl. Instr. Meth. Phys. Res. B* **360** 30
- [19] Ferrari A C 2007 *Solid State Commun.* **143** 47
- [20] Ona S, Nakamoto Y, Kagayama T, Shimizu K, Nishikawa Y, Murakami M, Kusakabe K, Watanuki T and Ohishi Y 2008 *J. Phys.: Conf. Series* **121** 062006
- [21] Yadav V S, Sahu D K, Singh M and Kumar K 2009 *Proc. WCECS I* (San Francisco USA)